International Journal of Heat and Mass Transfer 52 (2009) 1600–1607

Contents lists available at ScienceDirect

International Journal of Heat and Mass Transfer

journal homepage: www.elsevier.com/locate/ijhmt

Transient heat conduction in rolling/sliding components by a dual reciprocity boundary element method

Jun Wen, M.M. Khonsari *

Louisiana State University, Department of Mechanical Engineering, 2508 Patrick Taylor Hall, Baton Rouge, LA 70808, USA

ARTICLE INFO

Article history:
Received 13 February 2008
Received in revised form 16 July 2008
Available online 14 October 2008

Keywords:
Transfer matrix method
Dual reciprocity boundary element method
Transient heat conduction
Moving heat source

ABSTRACT

A transfer matrix method associated with the dual reciprocity boundary element method (DRBEM) is developed for the study of transient heat conduction problems in presence of moving heat sources. In this method, the time integration is processed by an iteration transfer matrix method, the coefficient matrices are calculated only once, and no domain integration is required. It is shown that the application of DRBEM results in considerable savings in computation time and data preparation. Numerical examples are presented to demonstrate the efficiency and accuracy of the method by comparing the computed results with either published results or solutions using the finite element method. While only two-dimensional problems are presented in the paper, the method can be readily extended to three-dimensional problems to handle more complicated contact problems.

© 2009 Published by Elsevier Ltd.

1. Introduction

Moving heat source problems occur in a wide variety of industrial applications where two surfaces are in relative sliding motion. Examples include the interaction of the rolling elements and races in roller bearings, shafts in journal bearings, and steel rolls in rolling mills, where the interacting bodies undergo one or more moving heat sources due to rubbing. Relative to the heat source, the stationary body – the outer race of a roller bearing or the sleeve of a journal bearing – is subjected to a fixed heat source. The sliding body – the roller and the shaft that experience moving heat source – is periodically heated over a small contact surface area while cooled over all or part of surface area by convention.

There are volumes of published papers dealing with the thermal behavior of rotating cylinder subjected to surface heating and convective cooling. The classic work was done by Jaeger [1], who developed an analytical transient solution for an adiabatic cylinder subject a rotating heat source on its surface. DesRuisseaux and Zerkle [2] extended Jaeger's solution by assuming that a convective cooling occurs over the entire cylindrical surface. Ling et al. [3] outlined the quasi-stationary solution for a cylinder subject to cooling and heating. Patula [4] presented a quasi-stationary solution related to cold rolling with the cylinder cooled and heated on parts of its surface but insulated on the rest. Yuen [5] extended the boundary condition formulation to nonuniform heating and cooling, but without presenting nonuniform cooling case. Ulysse and Khonsari [6] developed an analytical solution for steady-state temperature distribution in a cylinder undergoing uniform heating and nonuniform cooling. By neglecting the axial heat conduction due to high rotation speed, Gecim and Winer [7,8] presented the steady temperature solution in a rotating cylinder subject to surface heating and convective cooling. All these temperature models are analytical in nature. To facilitate such treatment, many simplifying assumptions had to be made.

In addition to the analytical solutions, significant efforts have been devoted to study thermal behavior of rotating cylinder by numerical techniques. Tseng [9] used a first-order upwind differencing scheme to study the steady-state heat transfer behavior of a two-dimensional rotating roll. Bennon [10] developed a three-dimensional finite difference model to predict the temperature distribution of the work roll in both axial and circumferential directions. Hwang et al. [11] performed a two-dimensional finite element analysis of steady-state heat transfer that included staggered thermomechanical coupling. Lee et al. [12] presented a three-dimensional finite element solution to the heat transfer problem in hot rolling operation. For the finite element method and the finite difference analysis, a very fine mesh is generally required to obtain an accurate temperature solution because the high temperature gradient is localized in a thin layer near the surface.

Compared to the finite element method and the finite difference method, the most important feature of the boundary element method is that it only requires discretization of the boundary rather than that of the whole volume, which reduces the dimensionality of the problem by one. There are many published papers where researchers apply the boundary element method to solve

* Corresponding author.
E-mail address: Khonsari@me.lsu.edu (M.M. Khonsari).

0017-9310/$ - see front matter © 2009 Published by Elsevier Ltd.
doi:10.1016/j.ijheatmasstransfer.2008.07.039

Nomenclature

$\mathbf{A}$	coefficient matrix for TMM
B	Biot number, $B = hR/k$
$\mathbf{B}$	assembled boundary integral matrix related to field unknowns
$\mathbf{B}'$	modified $\mathbf{B}$ matrix, $\mathbf{B}' = \mathbf{B}\mathbf{F}'\mathbf{F}^{-1}$
$c(\xi)$	constant in the boundary integration equation
$\mathbf{C}$	matrix defined by $\mathbf{C} = \frac{1}{\alpha}\{\mathbf{H}\widehat{\mathbf{T}} - \mathbf{G}\widehat{\mathbf{Q}}\}F^{-1}$
$\mathbf{D}$	assembled boundary integral matrix related to known boundary temperature or flux
$f_j(\mathbf{x})$	interpolation functions (distance functions)
$\mathbf{F}$	square matrix, $F_{ij} = f_j(\mathbf{x}_i)$
$\mathbf{F}'(\mathbf{x})$	modified $\mathbf{F}$ matrix defined in Eq. (24b)
$\mathbf{G}$	matrix of boundary integrals with kernel $\widetilde{T}$
h	heat transfer coefficient (W/m^2 K)
$\mathbf{H}$	matrix of boundary integrals with kernel $\tilde{q}$
$\mathbf{I}$	identity matrix
k	thermal conductivity (w/m K)
$\mathbf{M}$	coefficient matrix for TMM related to boundary conditions
n	unit normal outward to the boundary
N_B, N_I	number of boundary and internal nodes
N_{mov}	number of moving steps in one cycle
Pe	Peclet number, $Pe = \omega R^2/\alpha$
$\bar{q}$	prescribed boundary flux (W/m^2)
$\tilde{q}(\mathbf{x}), \hat{q}_j(\mathbf{x})$	heat flux from fundamental solution, and heat flux related to DRBEM (W/m^2)
$\mathbf{Q}, \hat{\mathbf{q}}_j$	nodal vector of q, and nodal vector of $\hat{q}_j$
$\widehat{\mathbf{Q}}$	matrix of vectors $\hat{\mathbf{q}}_j$
r_j	distance between the field point $\mathbf{x}$ and the collocation points $\mathbf{x}_j$, $r_j = \|\mathbf{x} - \mathbf{x}_j\|$ (m)
R	radius of cylinder (m)
$\mathbf{R}(t)$	vector of known boundary conditions
$T, \overline{T}, T^{(0)}, T_\infty$	field temperature, prescribed boundary temperature, initial temperature, and ambient temperature (°C)
$\widetilde{T}(\mathbf{x}), \widehat{T}_j(\mathbf{x})$	fundamental solution, and temperature related to DRBEM (°C)
$\mathbf{T}, \widehat{\mathbf{T}}_j$	nodal temperature vector of T, and nodal temperature vector of $\widehat{T}_j$
$\widehat{\mathbf{T}}$	matrix of vectors $\widehat{\mathbf{T}}_j$
υ	moving velocity (m/s)
$\mathbf{x}$	coordinate vector of field point (m)
$\mathbf{X}(t)$	vector of field unknowns
α	thermal diffusivity (m^2/s)
$\alpha_j(t)$	unknown time-dependant functions
$\boldsymbol{\alpha}$	vector of $\alpha_j(t)$
$\phi(t)$, ϕ_0	angular displacement, and angular semi-heating width (rad)
τ	time step size (s)
ξ	coordinate vector of source point (m)

Superscripts

-1	matrix inversion
$\cdot$	time derivative
k	time index

Subscripts

i	index of node or moving step
j	collocation index

the convective-diffusion equation for quasi-steady moving heat source problems. See, for example, papers dealing with the constant velocity machining or welding process [13–18]. It has been reported that using the BEM scheme, the convection term can be modeled with high precision than that by upwind differencing in finite difference, the sharp temperature gradient over the domain can be easily captured [13]. However, the presence of domain integrals makes the BEM inefficient when the method is applied to diffusion problems with source terms.

One of the most frequently used techniques for converting the domain integral into a boundary one is the so-called dual reciprocity boundary element method (DRBEM). This method was initially developed by Nardini and Brebbia [19] in the analysis of elastodynamics. It has been extended to deal with a variety of other problems [20–24]. However, when dealing with transient heat conduction, a temporal derivative is involved and a time marching schemes is generally required, which can be quite time consuming when the solution for large duration of time is desired. Zhu et al. [25] showed an efficient methodology called the Laplace transform dual reciprocity method (LTDRM) for problems involving time marching. Amado et al. [26] studied the application of the LTDRM in the modeling of the laser heat treatment. They showed that while the lengthy computations for a large time marching scheme are avoided, a large number of Laplace solutions is needed to obtain a reliable inversion from the Laplace domain temperature to the time one, particularly when pulse-like thermal cycles are induced.

Vick et al. [27] developed a boundary element model to analyze the surface temperatures generated by friction in sliding contact, and in the subsequent study [28] applied it to examine the effects of surface coatings on the temperatures produced by friction due to sliding contact. A moving full space Green's function was used as the fundamental solution in both studies. It was a time-dependant fundamental solution approach, Scheme 2 in Ref. [29], where the time integration was performed within the entire span of time interval between the initial time and the desired time level. Although in this approach the time integration still needs to be carried out, if the span of time integration is quite large, no temperature values at internal nodes need to be computed and stored at each intermediate time step. This method may yield saving of computational time if no unknown temperature values are needed at intermediate time steps. However, if the temperature variations up to steady state are of interest, this method becomes time consuming because the time integration always restarts from the initial time for the temperatures at every desired time.

A survey of the literature reveals that there is very little published research on the application of DRBEM dealing with the heat conduction in the rolling elements, especially when they are subjected to an oscillating motion such as in the so-called pin-joint assembly found in heavy construction and earth-moving machines. In this paper, a transfer matrix method associated with the DRBEM is developed for the study of transient heat conduction problems in presence of moving heat sources. In this method, the time integration is processed by an iteration transfer matrix method, the coefficient matrices are calculated only once, and no domain integration is required. It is shown that the application of DRBEM results in considerable savings in computation time and data preparation. Numerical examples are presented to demonstrate the efficiency and accuracy of the method by comparing the computed results with either published results or solutions using the finite element method. While only two-dimensional problems are presented in the paper, the method can be readily extended to three-dimensional problems to handle more complicated contact problems.

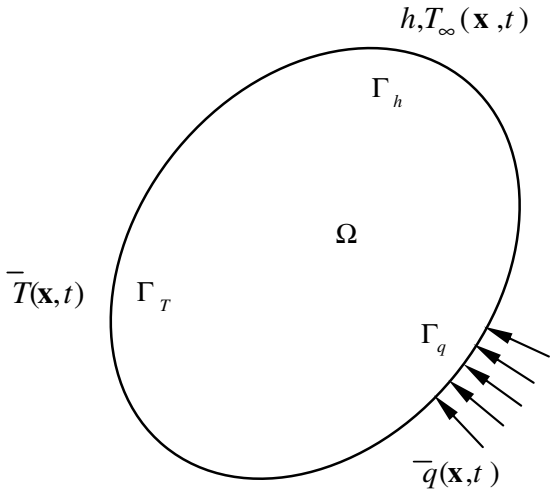

Fig. 1. Problem configuration.

2. Formulation

Consider a transient temperature field $T(\mathbf{x},t)$ in a domain Ω with a boundary $\Gamma = \Gamma_T \cup \Gamma_q \cup \Gamma_h$ shown in Fig. 1. The equation governing the heat conduction is:

$$\nabla^2 T(\mathbf{x},t) = \frac{1}{\alpha}\dot{T}(\mathbf{x},t), \qquad \mathbf{x} \in \Omega, \quad t > 0 \tag{1}$$

with the initial condition

$$T(\mathbf{x},0) = T^{(0)}(\mathbf{x}), \quad \mathbf{x} \in \Omega \tag{1a}$$

and the boundary conditions are given by

$$\text{Dirichlet}: \quad T(\mathbf{x},t) = \overline{T}(\mathbf{x},t), \quad \mathbf{x} \in \Gamma_T \tag{1b}$$
$$\text{Neumann}: \quad q(\mathbf{x},t) = \bar{q}(\mathbf{x},t), \quad \mathbf{x} \in \Gamma_q \tag{1c}$$
$$\text{Robin}: \quad q(\mathbf{x},t) = h(T_\infty - T), \quad \mathbf{x} \in \Gamma_h \tag{1d}$$

where $\mathbf{x}$ is the coordinate vector. The parameter t denotes the time, and the super-dot stands for the derivative with respect to time. α is the thermal diffusivity of the material. $q(\mathbf{x},t)$ is the heat flux defined as $q(\mathbf{x},t) = k\frac{\partial T}{\partial n}$, where k is the thermal conductivity of the material, and n is the unit normal outward to the boundary Γ. $T^{(0)}(\mathbf{x})$ represents the initial temperature distribution. $\overline{T}(\mathbf{x},t)$ and $\bar{q}(\mathbf{x},t)$ are the prescribed boundary temperature and flux, respectively. The parameter h is the heat transfer coefficient, and T_∞ stands for the ambient temperature.

In the dual reciprocity formulation [21], the temperature is approximated in the following manner:

$$T(\mathbf{x},t) \approx \sum_{j=1}^{N_B+N_I} \alpha_j(t) f_j(\mathbf{x}) \tag{2}$$

where N_B is the number of boundary nodes defining the discretization of the boundary Γ, and N_I is the number of internal nodes. The $N_B + N_I$ different nodes make up of the DRM collocation points. $\alpha_j(t)$ are the unknown time-dependant functions. $f_j(\mathbf{x})$ are known interpolation functions linked to a set of particular solutions $\widehat{T}_j(\mathbf{x})$ through the relation

$$\nabla^2 \widehat{T}_j(\mathbf{x}) = f_j(\mathbf{x}), \quad j = 1,2,\ldots,N_B+N_I \tag{3}$$

where $\widehat{T}_j(\mathbf{x})$ can be interpreted as a pseudo-temperature with an associated heat flux defined on the boundary as $\hat{q}_j(\mathbf{x}) = k\frac{\partial \widehat{T}_j(\mathbf{x})}{\partial n}$. $f_j(\mathbf{x})$ is chosen to be the distance functions, e.g. $f_j(\mathbf{x}) = 1 + r_j$ in the current study with $r_j = \|\mathbf{x} - \mathbf{x}_j\|$ being the distance between the field point $\mathbf{x}$ and the collocation points $\mathbf{x}_j$.

Evaluating Eq. (3) at every points $\mathbf{x}_i$, $i = 1,2,\ldots,N_B + N_I$, the resulting set of equations can be expressed in matrix form as

$$\mathbf{T} = \mathbf{F}\boldsymbol{\alpha} \tag{4}$$

where $\mathbf{T} = \{T_i\}$ is the nodal temperature vector of T, and $\boldsymbol{\alpha} = \{\alpha_j\}$ is a unknown vector. $\mathbf{F}$ is a square matrix with its entries defined as $F_{ij} = f_j(\mathbf{x}_i)$.

Taking derivative of Eq. (4) with respect to time yields

$$\dot{\mathbf{T}} = \mathbf{F}\dot{\boldsymbol{\alpha}} \tag{5}$$

Inversion of Eq. (5) results in

$$\dot{\boldsymbol{\alpha}} = \mathbf{F}^{-1}\dot{\mathbf{T}} \tag{6}$$

where superscript -1 denotes the matrix inversion.

Applying the usual dual reciprocity procedure [21], i.e. substituting Eq. (2) into Eq. (1), the result is multiplied by the steady-state fundamental solution $\widetilde{T}$, and then integrating twice by parts or using Green's second identity, yields the standard DRBEM integral equation:

$$\begin{aligned} c(\xi)T(\xi,t) + \int_\Gamma \tilde{q}(\xi,\mathbf{x})T(\mathbf{x},t)\,d\Gamma(\mathbf{x}) - \int_\Gamma \widetilde{T}(\xi,\mathbf{x})q(\mathbf{x},t)\,d\Gamma(\mathbf{x}) \\ = \frac{1}{\alpha}\sum_{j=1}^{N_B+N_I}\dot{\alpha}_j(t)\left\{c(\xi)\widehat{T}_j(\xi) + \int_\Gamma \tilde{q}(\xi,\mathbf{x})\widehat{T}_j(\mathbf{x})\,d\Gamma(\mathbf{x}) \right. \\ \left. - \int_\Gamma \widetilde{T}(\xi,\mathbf{x})\hat{q}_j(\mathbf{x})\,d\Gamma(\mathbf{x})\right\} \end{aligned} \tag{7}$$

where ξ is the current point located on the boundary or within the domain Ω. $c(\xi) = 1$ when ξ is within the domain. Otherwise, it is equal to the fraction of the angle with vertex at ξ subtended within the domain. $\tilde{q}(\mathbf{x})$ is defined as $\tilde{q}(\mathbf{x}) = k\frac{\partial T(\mathbf{x})}{\partial n}$.

Using the standard boundary element discretization procedure [20], i.e. the local approximation of both the shape of the boundary and the distributions of appropriate functions within boundary elements, the application of Eq. (7) at the boundary and internal nodes ξ_i, $i = 1,2,\ldots,N_B + N_I$, results in the following systems of equations in the matrix form as:

$$\mathbf{HT} - \mathbf{GQ} = \frac{1}{\alpha}\sum_{j=1}^{N_B+N_I}\dot{\alpha}_j(t)\left\{\mathbf{H}\widehat{\mathbf{T}}_j - \mathbf{G}\hat{\mathbf{q}}_j\right\} \tag{8}$$

where $\mathbf{H}$ and $\mathbf{G}$ are the matrices of boundary integrals with kernels $\tilde{q}$ and $\widetilde{T}$, respectively. $\mathbf{T}$ and $\mathbf{Q}$ are nodal vectors of T and q, respectively; $\widehat{\mathbf{T}}_j$ and $\hat{\mathbf{q}}_j$ are nodal vectors of $\widehat{T}_j$ and $\hat{q}_j$, respectively. Note that the term $c(\xi)$ has been placed on the leading diagonal of matrix $\mathbf{H}$. The matrix $\mathbf{T}$ contains temperature at both internal and boundary nodes. The heat flux $\mathbf{q}$ is associated with the boundary nodes, but not with the internal nodes. The internal nodes are not always needed. When introduced, they are independent of each other, i.e. there is no internal mesh.

Collecting $\widehat{\mathbf{T}}_j$ and $\hat{\mathbf{q}}_j$ vectors in Eq. (8) into matrices, and dropping the summation yields:

$$\mathbf{HT} - \mathbf{GQ} = \frac{1}{\alpha}\left\{\mathbf{H}\widehat{\mathbf{T}} - \mathbf{G}\widehat{\mathbf{Q}}\right\}\dot{\boldsymbol{\alpha}} \tag{9}$$

Substituting Eq. (6) into Eq. (9) results in

$$\mathbf{HT} - \mathbf{GQ} = \mathbf{C}\dot{\mathbf{T}} \tag{10a}$$

with

$$\mathbf{C} = \frac{1}{\alpha}\left\{\mathbf{H}\widehat{\mathbf{T}} - \mathbf{G}\widehat{\mathbf{Q}}\right\}F^{-1} \tag{10b}$$

By applying the prescribed boundary conditions in Eqs. (1b)–(1d), Eq. (10a) can be rewritten in the following form:

$$\mathbf{BX}(t) = \mathbf{DR}(t) + \mathbf{C}\dot{\mathbf{T}}(t) \tag{11}$$

where $\mathbf{X}(t)$ contains the unknown nodal values of temperature for the Neumann or the Robin boundary nodes, and heat flux for the Dirichlet boundary nodes. $\mathbf{R}(t)$ contains the known nodal values of temperature or heat flux for the Dirichlet or the Neumann boundary nodes. For the Robin boundary nodes, T_∞ is stored and the corresponding columns of the matrix $\mathbf{G}$ are multiplied by h. Matrices $\mathbf{H}$, $\mathbf{G}$ and $\mathbf{C}$ are only dependent upon the model geometry, and thus they are needed to be calculated only once. The matrices $\mathbf{B}$ and $\mathbf{D}$ are composed of the columns of the matrices $\mathbf{G}$ and $\mathbf{H}$, depending on the prescribed boundary conditions.

Eq. (11) represents a system of equations of mixed type because $\mathbf{X}(t)$ may include both the unknown temperature and heat flux depending on the boundary conditions. In what follows, we first obtain a general solution to Eq. (11) subject to different boundary conditions given in Eqs. (1b)–(1d) and subsequently extend the method to the moving boundary problems.

2.1. Neumann and Robin boundary conditions

When the boundary conditions are only of Neumann and Robin type, $\mathbf{X}(t)$ contains only unknown temperature. Then Eq. (11) can be rewritten in the form of

$$\mathbf{BT}(t) = \mathbf{DR}(t) + \mathbf{C}\dot{\mathbf{T}}(t) \tag{12}$$

The solution of Eq. (12) is [30]:

$$\mathbf{T}(t) = \exp(\mathbf{C}^{-1}\mathbf{B}t)T^{(0)} - \int_0^t \exp[\mathbf{C}^{-1}\mathbf{B}(t-s)]\mathbf{C}^{-1}\mathbf{DR}(s)\,ds \tag{13}$$

Let t_k and $t_{k+1} = t_k + \tau$ be the time instants of two continuous steps k and $k+1$, respectively. Then, referring to Eq. (13) the temperature at time t_k can be obtained as:

$$\mathbf{T}^{(k)} = \exp(\mathbf{C}^{-1}\mathbf{B}t_k)\mathbf{T}^{(0)} - \int_0^{t_k} \exp[\mathbf{C}^{-1}\mathbf{B}(t_k-s)]\mathbf{C}^{-1}\mathbf{DR}(s)\,ds \tag{14}$$

Hence, the temperature at time t_{k+1} is:

$$\begin{aligned}\mathbf{T}^{(k+1)} &= \exp\left(\mathbf{C}^{-1}\mathbf{B}t_{k+1}\right)\mathbf{T}^{(0)} - \int_0^{t_{k+1}} \exp\left(\mathbf{C}^{-1}\mathbf{B}(t_{k+1}-s)\right)\mathbf{C}^{-1}\mathbf{DR}(s)\,ds \\ &= \exp(\mathbf{C}^{-1}\mathbf{B}\tau)\mathbf{T}^{(k)} - \int_0^{\tau} \exp(\mathbf{C}^{-1}\mathbf{B}(\tau-s))\mathbf{C}^{-1}\mathbf{DR}(t_k+s)\,ds\end{aligned} \tag{15}$$

Whether the integrand in Eq. (15) is analytically integrable or not depends on the expression of the prescribed boundary conditions $\mathbf{R}(t)$. If not analytically integrable, a small time step τ must be chosen such that from time t_k to t_{k+1}, $\mathbf{R}(t)$ can be treated to be constant, equal to its value at time t_k, i.e. $\mathbf{R}^{(k)}$. Then, performing the related integration [30], Eq. (15) yields

$$\mathbf{T}^{(k+1)} = \mathbf{AT}^{(k)} + \mathbf{MR}^{(k)} \tag{16}$$

with

$$\mathbf{A} = \exp(\mathbf{C}^{-1}\mathbf{B}\tau) \tag{16a}$$

$$\mathbf{M} = (\mathbf{I} - \mathbf{A})\mathbf{B}^{-1}\mathbf{D} \tag{16b}$$

where $\mathbf{I}$ is the identity matrix. The parameters $\mathbf{A}$ and $\mathbf{M}$ are the coefficient matrices. For a constant step size τ, they are constants and need to be calculated only once.

Eq. (16) is the iteration solution for the transfer matrix method. Starting from the initial temperature $\mathbf{T}^{(0)}$, the temperature $\mathbf{T}(\mathbf{x},t)$ at each time instant t_k can be calculated efficiently until the desired time level is reached. For the system that reaches the steady state after long enough time period, $\mathbf{A}$ in Eq. (16a) approaches to zero when giving a large enough value of τ, and thus Eq. (16) becomes:

$$\mathbf{T}^{(ss)} = \mathbf{B}^{-1}\mathbf{DR} \tag{17}$$

where $\mathbf{T}^{(ss)}$ represents the node temperatures at the steady state. Eq. (17) is consistent with the steady-state solution derived from Eq. (12) when $\dot{\mathbf{T}}(t) = 0$.

The important step is to evaluate the matrix exponential $\mathbf{A}$ accurately, for which the so-called precise time integration (PTI) proposed by Zhong and Williams [31] is used. The method, which is unconditionally stable, uses the 2^N algorithm described as follows. Let $N = 20$, $m = 2^N = 1{,}048{,}576$, then $\Delta\tau = \tau/m$ is an extremely small time interval. Using the superposition of exponential function:

$$A = \exp(\mathbf{C}^{-1}\mathbf{B}\tau) = [\exp(\mathbf{C}^{-1}\mathbf{B}\cdot\Delta\tau)]^{2^N} \tag{18}$$

and the Taylor expansion:

$$\begin{aligned}\exp(\mathbf{C}^{-1}\mathbf{B}\cdot\Delta\tau) &\approx I + \mathbf{C}^{-1}\mathbf{B}\cdot\Delta t + \frac{(\mathbf{C}^{-1}\mathbf{B}\cdot\Delta t)^2}{2!} + \frac{(\mathbf{C}^{-1}\mathbf{B}\cdot\Delta t)^3}{3!} + \cdots \\ &+ \frac{(\mathbf{C}^{-1}\mathbf{B}\cdot\Delta t)^p}{p!} = I + A_a\end{aligned} \tag{19}$$

with

$$\mathbf{A}_a = \mathbf{C}^{-1}\mathbf{B}\cdot\Delta t + \frac{(\mathbf{C}^{-1}\mathbf{B}\cdot\Delta t)^2}{2!} + \frac{(\mathbf{C}^{-1}\mathbf{B}\cdot\Delta t)^3}{3!} + \cdots + \frac{(\mathbf{C}^{-1}\mathbf{B}\cdot\Delta t)^p}{p!} \tag{20}$$

results in

$$\mathbf{A} = (\mathbf{I} + \mathbf{A}_a)^{2^N} \tag{21}$$

Taking into account the relationship

$$(\mathbf{I} + \mathbf{A}_a)^2 = I + (2\mathbf{A}_a + \mathbf{A}_a\cdot\mathbf{A}_a) \tag{22}$$

it can be shown that, by substituting $\mathbf{A}_a$ by $(2\mathbf{A}_a + \mathbf{A}_a\cdot\mathbf{A}_a)$, $\mathbf{I} + \mathbf{A}_a$ becomes $\mathbf{I} + (2\mathbf{A}_a + \mathbf{A}_a\cdot\mathbf{A}_a) = (\mathbf{I} + \mathbf{A}_a)^2$, and $[\mathbf{I} + (2\mathbf{A}_a + \mathbf{A}_a\cdot\mathbf{A}_a)]^2 = \left[(\mathbf{I} + \mathbf{A}_a)^2\right]^2 = (\mathbf{I} + \mathbf{A}_a)^{2^2}$. Repeating such substitution for N times yields the solution of Eq. (21).

It is noted that the matrix $\mathbf{A}_a$ is small compared to identity matrix $\mathbf{I}$ due to a very small time interval $\Delta\tau$. When calculating matrix $\mathbf{A}$ by the above algorithm, first N times of substitution is executed to the small matrix $\mathbf{A}_a$ and then the result is added to the identity matrix $\mathbf{I}$, which avoids the direct additions of the identity matrix $\mathbf{I}$ and small matrix, and thus the loss of significant digits during the computations.

Alternatively, Chen et al. [32] propose an adaptive PTI algorithm, which determines the value of N and p adaptively based on the problem characteristics and the prescribed computational error tolerance. It saves much computer time for calculating matrix $\mathbf{A}$. In this paper, the adaptive PTI algorithm is used to evaluate the coefficient matrices.

2.2. Dirichlet boundary conditions

If the problem is subject to Dirichlet boundary condition, $\mathbf{X}(t)$ in Eq. (11) includes both the unknown temperature and heat flux, and Eq. (11) becomes a system of equations of mixed type, which require a special treatment as follows.

From Eq. (2), the heat flux on the boundary where the Dirichlet boundary condition is prescribed can obtained as [33]

$$q(\mathbf{x},t) \approx k\sum_{j=1}^{N_B+N_I} \alpha_j(t)\frac{\partial f_j(\mathbf{x})}{\partial n} \tag{23}$$

then the vector of unknowns $\mathbf{X}(t)$ in Eq. (11) can be expressed as

$$\mathbf{X}(t) = \mathbf{F}'(\mathbf{x})\boldsymbol{\alpha}(t) \tag{24a}$$

where $\mathbf{F}'(\mathbf{x})$ is similar to F in Eq. (4) except that the entries corresponding to the Dirichlet boundary nodes $\mathbf{x}_i$ become $k\frac{\partial f_j(\mathbf{x}_i)}{\partial n}$ instead of $f_j(\mathbf{x}_i)$, that is:

$$\mathbf{F}'(\mathbf{x}) = \begin{cases} f_j(\mathbf{x}_i) & \text{Neumann or Robin boundary condition is prescribed at node } \mathbf{x}_i \\ k\frac{\partial f_j(\mathbf{x}_i)}{\partial n} & \text{Dirichlet boundary condition is prescribed at node } \mathbf{x}_i \end{cases} \tag{24b}$$

Inversion of Eq. (4) yields

$$\boldsymbol{\alpha} = \mathbf{F}^{-1}\mathbf{T} \tag{25}$$

Substitution of Eq. (25) into Eq. (24a) results in

$$\mathbf{X}(t) = \mathbf{F}'\mathbf{F}^{-1}\mathbf{T} \tag{26}$$

Applying Eq. (26), Eq. (11) can be expressed as

$$\mathbf{B}'\mathbf{T}(t) = \mathbf{D}\mathbf{R}(t) + \mathbf{C}\dot{\mathbf{T}}(t) \tag{27a}$$

with

$$\mathbf{B}' = \mathbf{B}\mathbf{F}'\mathbf{F}^{-1} \tag{27b}$$

Note that Eq. (27a) can be obtained by replacing $\mathbf{B}$ in Eq. (12) by $\mathbf{B}'$. Therefore, using the same method as in the previous case, Eq. (27a) can be solved.

2.3. Solution for moving boundary problems

In this section, the method is extended to solve the heat conduction equation subject to the moving heat source. Consider a body subject to the heat source $\bar{q}(\mathbf{x}, t)$ moving at velocity $\upsilon(t)$ along its boundary Γ. The moving cycle of the heat source is discretized into N_{mov} continuous steps such that within each step i ($i = 1,2,\ldots,N_{\text{mov}}$), the heat source can be treated to be stationary and acts on the body for time period τ_i, defined as:

$$\tau_i = \frac{\text{Moving distance in the } i\text{th step}}{\text{Average velocity in the } i\text{th step}} \tag{28}$$

Therefore, the problem within the time period τ_i is the same as that in Section 2.1 with the solution at the previous moving step $i-1$ within the time period τ_{i-1} as a pseudo-initial condition. Thus, the following iteration equation can be obtained:

$$\mathbf{T}^{(k+1)} = \mathbf{A}_i\mathbf{T}^{(k)} + \mathbf{M}_i\mathbf{R}^{(k)}, \quad i = 1,2,\ldots,N_{\text{mov}} \tag{29}$$

where $\mathbf{A}_i$ and $\mathbf{M}_i$ are the same as those in Eqs. (16a) and (16b). However, the matrices $\mathbf{B}$ and $\mathbf{D}$ are obtained by applying the corresponding boundary conditions within time period τ_i.

There are at most N_{mov} pairs of the coefficient matrices $\mathbf{A}_i$ and $\mathbf{M}_i$ to be evaluated. Each pair corresponds to a specified moving step of the heat source or a certain load condition on the boundary due to the motion of the flux. The calculations of different pairs of $\mathbf{A}_i$ and $\mathbf{M}_i$ are based on the same matrices $\mathbf{H}$ and $\mathbf{G}$ in Eq. (8) by using the corresponding boundary condition at the step i without introducing any additional boundary integration. According to different load steps due to the motion of the heat source, the matrices $\mathbf{A}_i$ and $\mathbf{M}_i$($i = 1,2,\ldots,N_{\text{mov}}$) are consecutively substituted into Eq. (29) to simulate the variations of the field temperature. It is noted that in one cycle, some pairs of $\mathbf{A}_i$ and $\mathbf{M}_i$ may be the same if heat source is subject to periodic sliding or oscillatory motion. In such case, less than N_{mov} pairs of different coefficient matrices are evaluated. Fig. 2 shows a flowchart of the main steps of the simulation algorithm for moving heat source problems.

Generally, the internal nodes in the DRBEM are not always needed [33]. However, it is noted that for the moving boundary problems, they are necessary no matter whether the boundary condition is of Dirichlet type or not [20,22]. In any event, even when internal nodes are introduced, they are independent of each other and thus no internal meshing would be required.

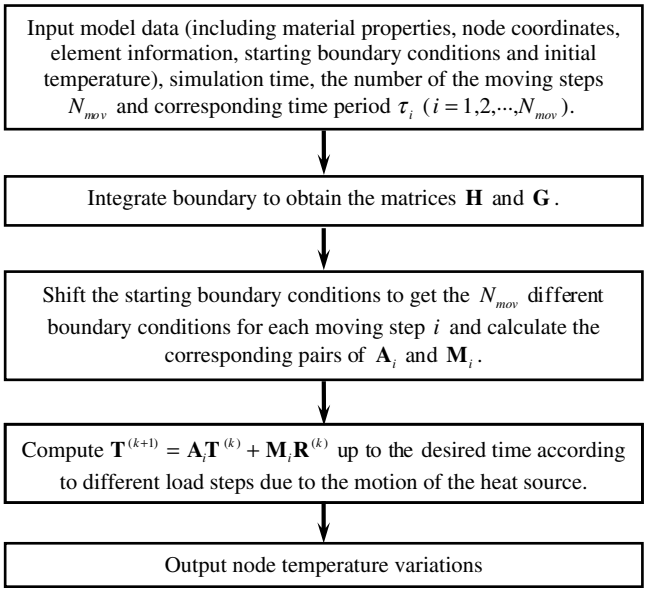

Fig. 2. A flowchart of the basic steps of the simulation algorithm for moving heat source problems.

3. Results and discussion

Based on the formulation described in Section 2, a computer program is developed to treat transient heat conduction problems with different types of boundary conditions [36–38]. The utility of the method is illustrated by application of the program to three problems. Examples are presented to validate the results and provide evidence for the efficiency and accuracy of the method.

3.1. Fixed boundary conditions

The first case involves the transient heat transfer in a square-shaped geometry shown in Fig. 3. The problem is treated as a two-dimensional problem by the present method although because of the nature of the boundary conditions, it could be trea-

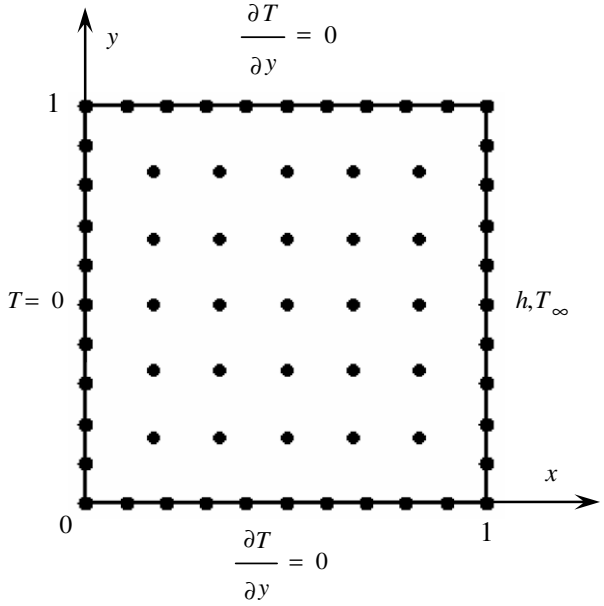

Fig. 3. Numerical model of the unit square.

ted as a one-dimensional problem. A Dirichlet boundary condition, $T = 0$ is applied at side $\mathbf{x} = 0$ and Robin boundary condition at side $\mathbf{x} = 1$ m with convective heat transfer coefficient $h = 1000\ \mathrm{W/m^2\ K}$ and ambient temperature $T_\infty = 20\ ^\circ\mathrm{C}$. The other two sides are subject to Neumann boundary conditions, $\bar{q} = 0$ (insulation). Zero initial temperature is assumed. The thermal conductivity of the material $k = 52\ \mathrm{W/m\ K}$, and the thermal diffusivity $\alpha = 10^{-5}\ \mathrm{m^2/s}$. The analytical solution for temperature distribution of such a problem can be derived [34] as

$$T(x,t) = \frac{HT_\infty}{1+H}\left\{x + 4\sum_{m=1}^{\infty}\frac{\beta_m\cos(\beta_m)-\sin(\beta_m)}{\beta_m[2\beta_m-\sin(2\beta_m)]}\exp\left(-\alpha\beta_m^2 t\right)\sin(\beta_m\mathbf{x})\right\} \tag{30}$$

where $H = h/k$, and β_m are the positive roots of equation $\beta_m\cot(\beta_m) = -H$.

As shown in Fig. 3, the boundary of the unit square is discretized into 40 equally sized linear elements with 40 boundary nodes, i.e. $N_B = 40$. To implement the Dirichlet boundary condition, 25 internal nodes are involved, i.e. $N_I = 25$. The comparison of temperature variation at location $\mathbf{x} = 1$, $y = 0.5$ by the present method along with the analytical solution is shown in Fig. 4(a). The comparison of temperature distribution between the present method and the analytical solution along the x-direction at $t = 10{,}000$ s is plotted in Fig. 4(b). It can be seen from Fig. 4 that the results from both methods agree very well. The time taken by the present method to do the simulation is comparable to the analytical solution on the same computer. Also the present method is unconditional stable. Changing the time step with different values, the exactly same results are obtained. When taking a large time step $\tau = 10{,}000$ s, the results shown in Fig. 4(b) are directly obtained by one step iteration. This feature is important for the moving boundary problem with variable velocity.

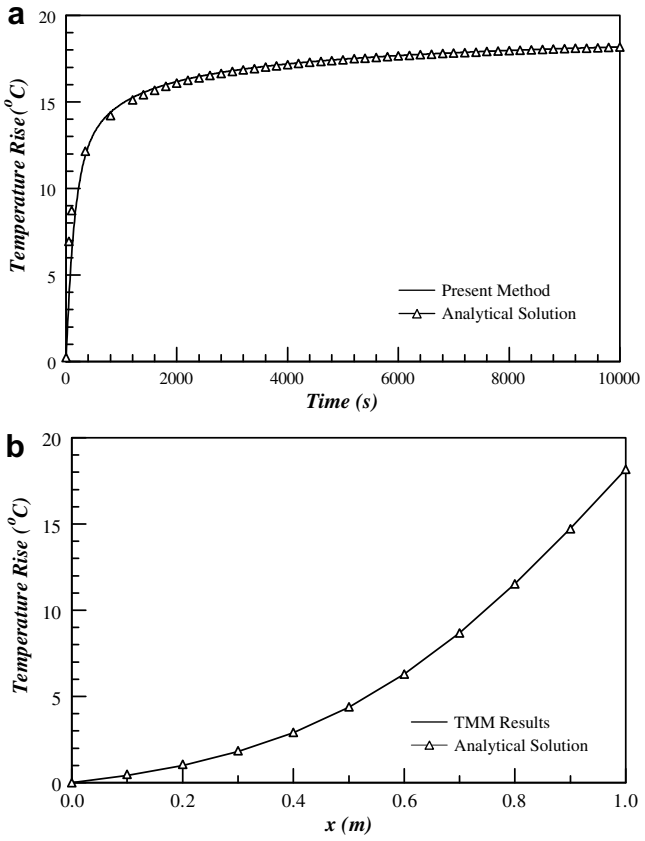

Fig. 4. (a) Comparison of temperature variation at location $\mathbf{x} = 1$, $y = 0.5$ by the present method along with the analytical solution. (b) Comparison of temperature distribution between the present method and the analytical solution along the x-direction at $t = 10{,}000$ s.

3.2. Unidirectional moving heat source

In this case, a long cylinder with radius R is subjected to a unidirectional moving heat source $\bar{q}$ along its surface with angular velocity $\dot{\phi}$. The heating is assumed to occur over the width $2\phi_0 = 0.2805$ rad. The rest of the surface is subjected to the convective boundary condition with heat transfer coefficient h and ambient temperature T_∞. The Peclet number $Pe = \dot{\phi}R^2/\alpha = 200$, and the Biot number $B = hR/k = 0.5$, here k and α are the thermal conductivity and the thermal diffusivity of the material, respectively.

The numerical model by the present method is shown in Fig. 5(a). There are 112 boundary nodes and 196 internal nodes, i.e. $N_B = 112$, $N_I = 196$. The boundary is discretized into 112 equally sized elements. In one cycle, the motion of the heat flux is divided into 112 steps, $N_{mov} = 112$, with the same time length $\tau = 2\pi/112\dot{\phi}$. Using the corresponding boundary condition within each step due to the flux motion, 112 pairs of coefficient matrices can be obtained. Substituting them into Eq. (29) and starting from the initial condition, temperature variations are simulated. For comparison, the finite element results are also presented. Fig. 5(b) shows the FEM model. It can be easily seen that the model scale is greatly reduced by the DRBEM compared with the FEM model.

The comparisons of the calculated results by the present method along with the results by ABAQUS are shown in Figs. 6 and 7. Fig. 6 presents the comparison of temperature distribution along the outer surface at steady state, Fig. 7(a) the comparison of the surface temperature variation up to 100 s, and Fig. 7(b) the comparison of the surface temperature variation in two cycles at steady state. All the results are in good agreement as shown in Figs. 6 and 7. In addition, the time taken by the present method is greatly less than that by ABAQUS for the same simulation on the same computer, i.e. 25 min for 1000 s simulation by the present method, while 2 h 18 min for 420 s simulation by ABAQUS. Such calculation efficiency will become more prominent when much longer time of temperature history is simulated. Most of time required by the present method is mainly in the calculation of the coefficient matrices A_i ($i = 1, 2, \ldots, N_{mov}$), i.e. the matrix exponential. Once the pairs of the coefficient matrices are determined, temperature variation can be obtained efficiently by the iteration equation (29).

3.3. Oscillating heat source

Considering the same example in Ref. [35] for the case of oscillating heat source, a rectangular domain 0.3×0.1 m is subject to an oscillating heat source $\bar{q}$ on its top surface with heating width 0.1 m and oscillation velocity $\upsilon = 1.2$ m/s. The rest of the surface is kept at constant temperature T_0. The initial temperature is T_i. The numerical model is shown in Fig. 8. 80 boundary nodes and 33 internal nodes are included. The top surface is discretized into 30 elements. The motion of the heat flux is divided into 40 steps in one cycle from the left to the right side. In every step the heat flux slides across one element size within time $\tau = 0.3/30/\upsilon = 0.00833$ s. One oscillation cycle includes 40 heating positions of the flux, i.e. $N_{mov} = 40$. However, there are only 21 different heating steps in one cycle, corresponding to 21 different load conditions from the left side to the right side. That is, some of the coefficient matrices are used twice in one cycle. Only the 21 pairs of coefficient matrices need to be evaluated by using Eqs. (16a) and (16b). Substituting them into Eq. (29) according to the oscillating motion of the heat source and starting from the initial condition, temperature variations are obtained.

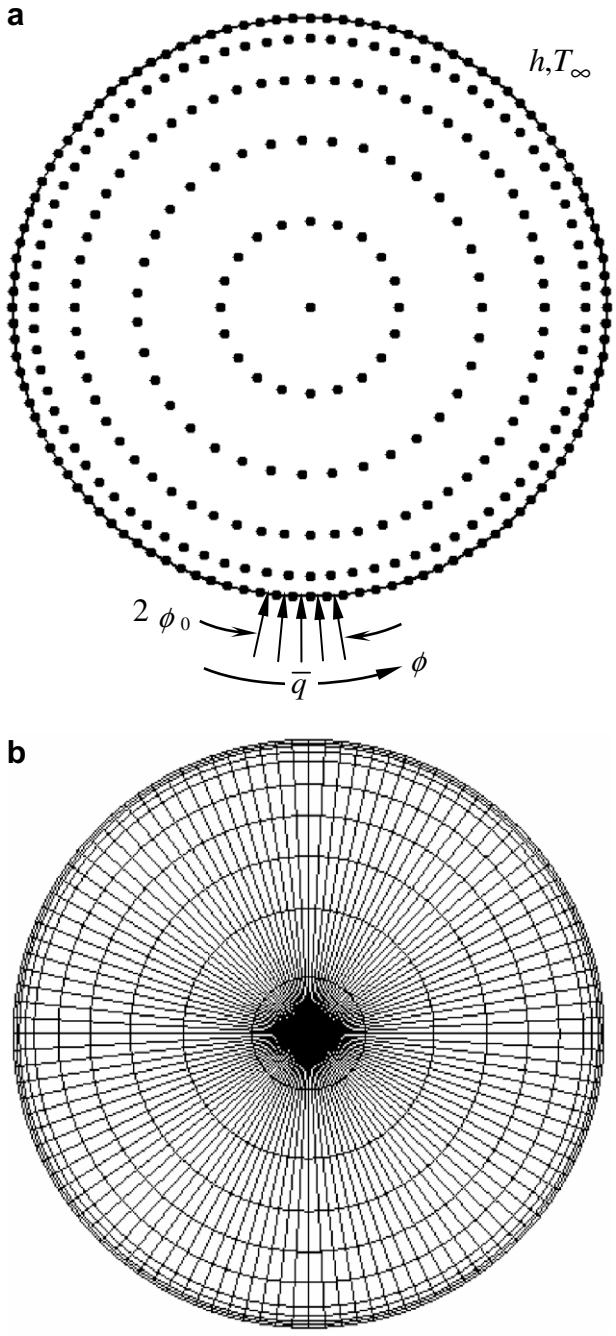

Fig. 5. Numerical model of the roller component. (a) BEM model and (b) FEM model.

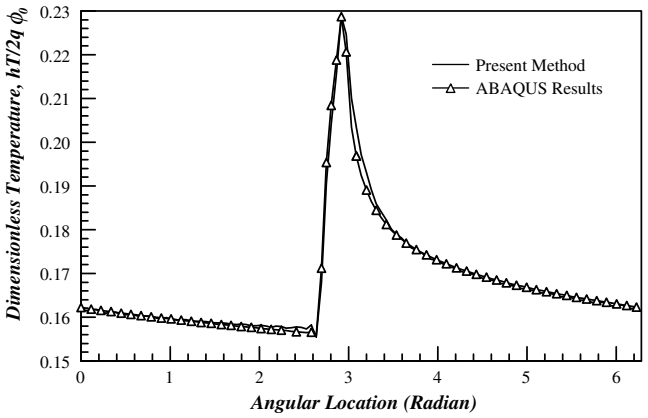

Fig. 6. Comparison of steady-state surface temperature distribution by the present method and ABAQUS.

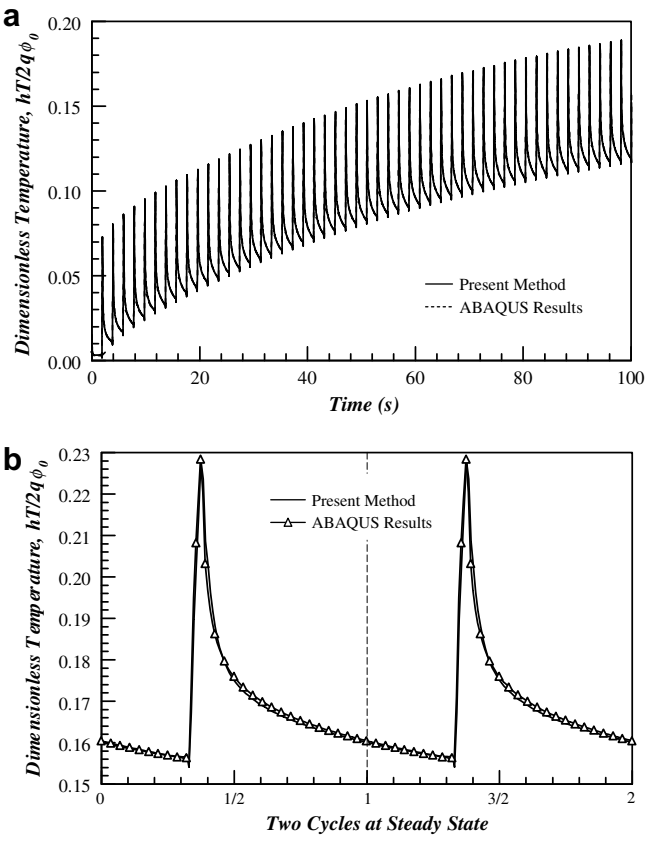

Fig. 7. (a) Comparison of surface temperature variation up to 100 s by the present method and ABAQUS. (b) Comparison of surface temperature variation in two cycles at steady state by the present method and ABAQUS.

The same parameters as in [35] are used in the simulation. Fig. 9 shows the comparison of the temperature rise by the present method and by the analytical solution at the locations (0.15,0.1), (0.05,0.1), (0.25,0.1) and (0.15,0.05). The both results are in good agreement. The results are efficiently obtained by the present method within 3 min, comparable to the analytical solution, whereas it required 11 h to accomplish the same task using the ABAQUS on the same computer.

4. Concluding remarks

In this study, a new method for transient heat conduction by a combination of the dual reciprocity boundary element method and the transfer matrix method is developed and applied to the study of problems in presence of moving heat sources. The proposed method avoids the use of the time marching schemes for transient problems and limits the discretization of the model to its boundary. Therefore, models based on this method considerably save the computational time and the date preparation.

Once the coefficient matrices are evaluated, the temperature variations can be efficiently simulated, and longer time of simulation does not increases much the time spending. This is important for the analysis of moving heat source problems, which generally takes a long time for the simulation to get to a steady state. Also the temporal derivative involved with transient problems is processed by a so-called precise time integration (PTI) method, which

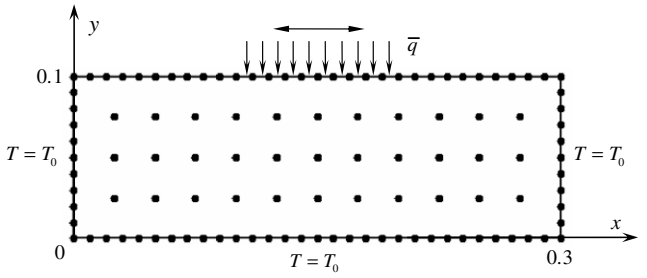

Fig. 8. Numerical model of a rectangular domain subject to an oscillating heat source.

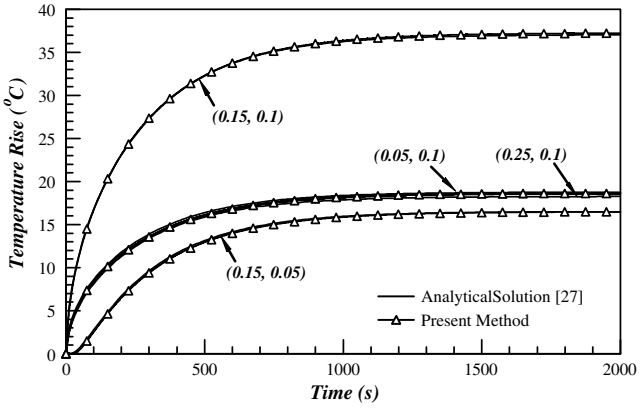

Fig. 9. Comparison of temperature rise obtained analytically and by the present method at locations (0.15, 0.1), (0.05, 0.1), (0.25, 0.1) and (0.15, 0.05).

makes the developed method unconditional stable, and thus makes it possible to use different time steps in the analysis and to efficiently simulate the moving heat source problems with variable velocity.

Numerical examples demonstrate the efficiency and accuracy of the method. The presented method provides an efficient solution for the moving heat source problems. In this work, only two-dimensional problems are presented. However, the procedure can be readily extended to three-dimensional problems as well as more complicated thermal contact problems. Also it is possible to use the method to treat problems with material nonlinearities by using the similar transformation as in Refs. [20,22,24,36]. It is noted that, due to the temperature-dependant material properties, the coefficient matrices **A** and **M** need to be calculated at each time step.

References

[1] J.C. Jaeger, Some problems involving line sources in conduction of heat, Philos. Mag. 35 (1944) 169–179.
[2] N.R. DesRuisseaux, R.D. Zerkle, Temperature in semi-infinite and cylinder bodies subjected to moving heat sources and surface cooling, ASME J. Heat Transfer 92 (1970) 456–464.
[3] F.F. Ling, W.M. Lai, D.A. Lucca, Fundamentals of Surface Mechanics with Applications, Springer, New York, NY, 1973. pp. 52–55.
[4] E.J. Patula, Steady-state temperature distribution in a rotating roll subject to surface heat fluxes and convective cooling, ASME J. Heat Transfer 103 (1981) 36–41.
[5] W.Y.D. Yuen, On the steady-state temperature distribution in a rotating cylinder subject to heating and cooling over its surface, ASME J. Heat Transfer 106 (1984) 578–585.
[6] P. Ulysse, M.M. Khonsari, Thermal response of rolling components under mixed boundary conditions: an analytical approach, ASME J. Tribol. 115 (1993) 857–865.
[7] B. Gecim, W.O. Winer, Steady temperature in a rotating cylinder subject to surface heating and convective cooling, ASME J. Tribol. 106 (1984) 120–127.
[8] B. Gecim, W.O. Winer, Steady temperature in a rotating cylinder – some variations in the geometry and the thermal boundary conditions, ASME J. Tribol. 108 (1986) 446–454.
[9] A.A. Tseng, Finite-difference solutions for heat transfer in a roll rotating at high speed, Numer. Heat Transfer 7 (1984) 113–125.
[10] W.D. Bennon, Evaluation of selective coolant application for the control of work roll thermal expansion, ASME J. Eng. Ind. 107 (1985) 146–152.
[11] S.M. Hwang, M.S. Joun, Y.H. Kang, Finite element analysis of temperatures, metal flow, and roll pressure in hot strip rolling, ASME J. Eng. Ind. 115 (1993) 290–298.
[12] J.D. Lee, M.T. Manzari, Y.L. Shen, W.J. Zeng, A finite element approach to transient thermal analysis of work rolls in rolling process, ASME J. Manuf. Sci. Eng. 122 (2000) 706–716.
[13] C.L. Chan, A. Chandra, A boundary element analysis of the thermal aspect of metal cutting process, ASME J. Eng. Ind. 113 (1991) 311–319.
[14] C.L. Chan, A. Chandra, An algorithm for handling corners in the boundary element method: application to conduction–convection equations, Appl. Math. Model. 15 (1991) 244–255.
[15] C.L. Chan, A. Chandra, A BEM approach to thermal aspects of machining processes and their design sensitivities, Appl. Math. Model. 15 (1991) 562–575.
[16] A. Chandra, C.L. Chan, A boundary element method for design sensitivities in steady-state conduction–convection problems, ASME J. Appl. Mech. 59 (1992) 190–192.
[17] A. Chandra, C.L. Chan, Thermal aspects of machining: a BEM approach, Int. J. Solids Struct. 31 (1994) 1657–1693.
[18] M. Hang, A. Okada, Computation of GMAW welding heat transfer with boundary element method, Adv. Eng. Softw. 16 (1993) 1–5.
[19] D. Nardini, C.A. Brebbia, A new approach to free vibration analysis using boundary elements, in: C.A. Brebbia (Ed.), Boundary Elements in Engineering, Springer, Berlin, 1982. pp. 312–326.
[20] L.C. Wrobel, C.A. Brebbia, The dual reciprocity boundary element formulation for nonlinear diffusion problems, Comput. Methods Appl. Mech. Eng. 65 (1987) 147–164.
[21] P.W. Partridge, C.A. Brebbia, Computer implementation of the dual reciprocity method for the solution of general field equations, Commun. Appl. Numer. Meth. 6 (1990) 83–92.
[22] P.W. Partridge, C.A. Brebbia, L.C. Wrobel, The Dual Reciprocity Boundary Element Method, Computational Mechanics Publications/Elsevier Applied Science, Southampton Boston/New York, 1992. pp. 175–195.
[23] J. Blobner, R.A. Białecki, G. Kuhn, Transient non-linear heat conduction–radiation problems – a boundary element formulation, Int. J. Numer. Meth. Eng. 46 (1999) 1865–1882.
[24] W.J. Minkowycz, E.M. Sparrow, J.Y. Murthy, Handbook of Numerical Heat Transfer, second ed., Wiley, Hoboken, NJ, 2006. pp. 142–155.
[25] S. Zhu, P. Satravaha, X. Lu, Solving linear diffusion equations with the dual reciprocity method in Laplace space, Eng. Anal. Bound. Elem. 13 (1994) 1–10.
[26] J.M. Amado, M.J. Tobar, A. Ramil, A. Yáñez, Application of the Laplace transform dual reciprocity boundary element method in the modelling of laser heat treatments, Eng. Anal. Bound. Elem. 29 (2005) 126–135.
[27] B. Vick, M.J. Furey, S.J. Foo, Boundary element thermal analysis of sliding contact, Numer. Heat Transfer 20 (1991) 19–40.
[28] B. Vick, L.P. Golan II, M.J. Furey, Thermal aspect due to surface films in sliding contact, ASME J. Tribol. 116 (1994) 238–246.
[29] C.A. Brebbia, J.C.F. Telles, L.C. Wrobel, Boundary Element Techniques: Theory and Application in Engineering, Springer, Berlin, 1984. pp. 156–164.
[30] A.D. Kraus, Matrices for Engineers, Oxford University Press, New York, 2002. pp. 241–246.
[31] W.X. Zhong, F.W. Williams, A precise time step integration method, Proc. Inst. Mech. Eng. C 208 (1994) 427–430.
[32] B.S. Chen, L.Y. Tong, et al., Transient heat transfer analysis of functionally graded materials using adaptive precise time integration and graded finite elements, Numer. Heat Transfer B 45 (2004) 181–200.
[33] R.A. Białecki, P. Jurgas, G. Kuhn, Dual reciprocity BEM without matrix inversion for transient heat conduction, Eng. Anal. Bound. Elem. 26 (2002) 227–236.
[34] M. Necati Özisik, Heat Conduction, second ed., Wiley, New York, NY, 1993. pp. 37–94.
[35] J. Wen, M.M. Khonsari, Analytical formulation for the temperature profile by Duhamel's theorem in bodies subjected to an oscillatory heat source, ASME J. Heat Transfer 129 (2007) 236–240.
[36] W.J. Minkowycz, E.M. Sparrow, Advances in Numerical Heat Transfer, vol. II, Taylor & Francis, New York, NY, 2000. pp. 146–152.
[37] X.W. Gao, T.G. Davies, Boundary Element Programming in Mechanics, Cambridge University Press, Cambridge, 2002. pp. 39–53.
[38] G. Beer, Programming the Boundary Element Method, Wiley, West Sussex, 2001. pp. 57–64.